INFLUENCE OF CURRENT EXCITATION PROFILES ON SCREENING-CURRENT EFFECTS IN REBCO BENDING MAGNETS FOR THE HEFEI ADVANCED LIGHT FACILITY

J. Xia*, Z. Bai, C. Chen, J. Xu, Z. Zhu, J. Zhao
University of Science and Technology of China, Hefei, China

Abstract

ReBCO coated conductors are promising for compact high-field bending magnets and are being considered for use in the Hefei Advanced Light Facility (HALF) to enhance the photon energy from bending-magnet radiation. However, screening-current effects induced during excitation remain an important issue for such magnets. In this work, these effects are investigated in the proposed bending magnet using the H-formulation. Several current excitation profiles with different ramping and holding stages are compared. The results show that the charging history strongly affects screening-current relaxation and the induced-field distribution. Under the present conditions, final holding at the operating current is more effective than a slow final ramp or distributed intermediate holding, providing guidance for optimizing charging schemes for future ReBCO bending magnets.

INTRODUCTION

ReBCO coated conductors are promising for compact high-field bending magnets because of their high current-carrying capability and excellent performance under strong magnetic fields. In the Hefei Advanced Light Facility (HALF), selected conventional dipole magnets are planned to be replaced by ReBCO high-temperature superconducting (HTS) bending magnets to enhance the photon energy from bending-magnet radiation [1].

However, screening currents are induced in ReBCO tapes during magnet excitation because of the large aspect ratio of coated conductors [2, 3]. The resulting screening-current-induced field (SCIF) can affect the magnetic-field behavior of the magnet and may lead to excitation-history-dependent field deviations. This effect needs to be carefully considered for storage-ring applications, where field stability and reproducibility are important.

In this study, screening-current effects in a HALF ReBCO bending magnet are simulated using the H-formulation. Several current excitation profiles with different ramping and holding stages are compared, including uniform ramping, fast ramping with final holding, fast-to-slow ramping, and stepwise excitation with intermediate holding. Their effects on screening-current relaxation and the resulting induced-field distribution are analyzed, providing guidance for optimizing charging schemes for future HTS bending magnets.

* waterx09@gmail.com

MAGNET CONFIGURATION AND SIMULATION SETUP

Magnet Configuration and Numerical Model

Figure 1 shows the two-dimensional cross-sectional model of the HTS bending magnet, which consists of an iron core, HTS coil regions, and an air domain. To reduce the computational cost, only one quarter of the cross section is modeled using geometric symmetry, and the multilayer ReBCO coated conductors are represented by equivalent homogeneous HTS domains [4]. The main operating parameters are summarized in Table 1.

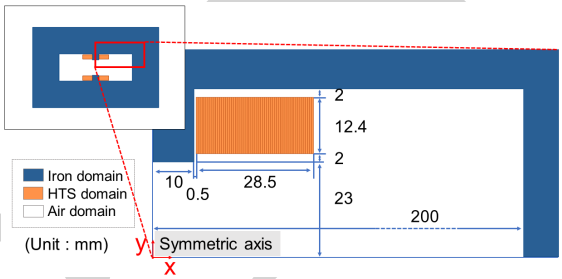

Figure 1: Two-dimensional cross-sectional model and geometric parameters of the HTS bending magnet.

Table 1: Main Operating Parameters of the Investigated ReBCO HTS Bending Magnet

Item	Unit	Value
Operating temperature, T_{op}	K	4.2
Operating current, I_{op}	A	270
Estimated critical current, I_c	A	385
Perpendicular field on conductor, $B_\perp$	T	5
Peak on-axis magnetic field, B_{peak}	T	6
On-axis field integral, $\int B_y dz$	T·m	0.368

The electromagnetic behavior of the HTS magnet is calculated using the H-formulation. The governing equation is written as

$$\nabla \times (\rho \nabla \times \mathbf{H}) + \mathbf{M}\frac{\partial \mathbf{H}}{\partial t} = 0, \quad (1)$$

where $\mathbf{H}$ is the magnetic field intensity, ρ is the electrical resistivity, and $\mathbf{M}$ represents the material-dependent magnetic constitutive relation [5]. The nonlinear magnetization of the iron core is included through the measured B–H curve. The ReBCO conductor is described by an E–J power-law relation, and the magnetic-field dependence of the critical current density J_{cB} is represented by a Kim-type

model. Thermal effects are neglected by assuming sufficient temperature margin.

In the two-dimensional model, the total current density in the HTS region is obtained as

$$J = \frac{\partial H_y}{\partial x} - \frac{\partial H_x}{\partial y}. \tag{2}$$

The screening-current density is then evaluated by subtracting the equivalent uniform transport-current density:

$$J_{sc} = J - J_t, \tag{3}$$

where $J_t = I(t)/S_{HTS}$, $I(t)$ is the transport current, and S_{HTS} is the HTS cross-sectional area.

In addition, the SCIF is defined as

$$B_{SCIF} = B_{total} - B_{transport}, \tag{4}$$

where B_{total} is obtained from the full electromagnetic solution and $B_{transport}$ is the magnetic field generated by the equivalent uniform transport-current density.

In this work, the quantities J_{sc}/J_{cB} and B_{SCIF} are used to evaluate the influence of different current excitation profiles.

Current Excitation Profiles

The current excitation profiles considered in this study are shown in Fig. 2. In all cases, the transport current is kept at 0 A during the first 60 s, and the operating current is 270 A.

Figure 2(a) compares three profiles with the same preparation time of 960 s: a uniform ramp at 0.3 A/s, a fast ramp at 3 A/s followed by final holding, and a fast-to-slow ramp with rates of 1.5 A/s and 0.15 A/s. Figure 2(b) further compares two holding strategies with the same total duration: final holding after a 0.3 A/s ramp and stepwise intermediate holding, where each 30 A current increase is followed by a 400-s holding stage. This comparison is used to examine the influence of holding-time distribution on screening-current relaxation.

RESULTS AND DISCUSSION

Figure 3 shows the temporal evolution of the normalized screening-current density. In Fig. 3(a), the fast ramp produces a large transient screening current, followed by continuous relaxation during the holding stage. The uniform ramp and the fast-to-slow ramp lead to similar residual screening-current levels, indicating that a slower final ramp does not clearly reduce the residual screening current under the present conditions.

Figure 3(b) further shows the influence of holding-time distribution. Although the screening current relaxes during each intermediate holding stage in the stepwise profile, subsequent current increases regenerate screening currents. Consequently, the residual screening-current level is higher than that obtained with final holding, suggesting that holding at the operating current is more effective than distributing the holding time during ramping.

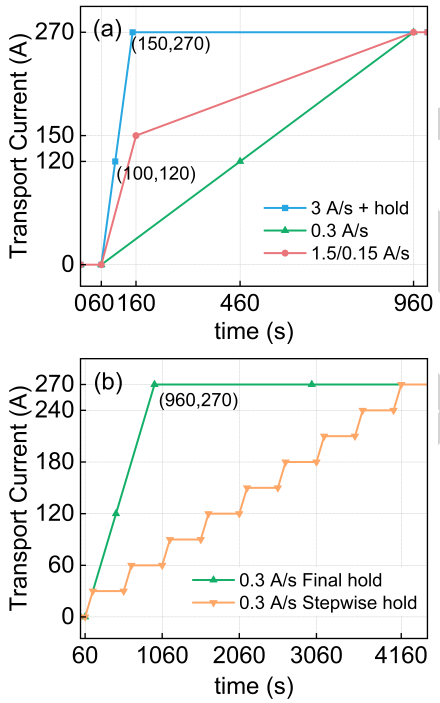

Figure 2: Current excitation profiles used in the simulations. (a) Three profiles with the same preparation time of 960 s: uniform ramp, fast ramp with final holding, and fast-to-slow ramp. (b) Comparison between final holding and stepwise intermediate holding.

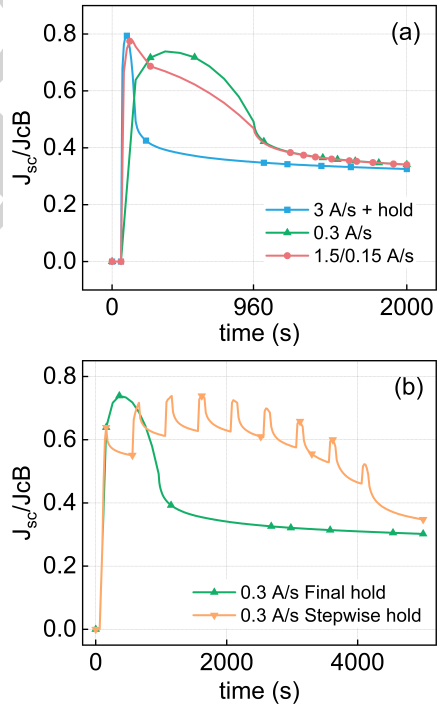

Figure 3: Temporal evolution of J_{sc}/J_{cB} under different excitation profiles. (a) Uniform ramp, fast ramp with final holding, and fast-to-slow ramp under the same preparation time of 960 s. (b) Final holding after a 0.3 A/s ramp and stepwise excitation with intermediate holding stages.

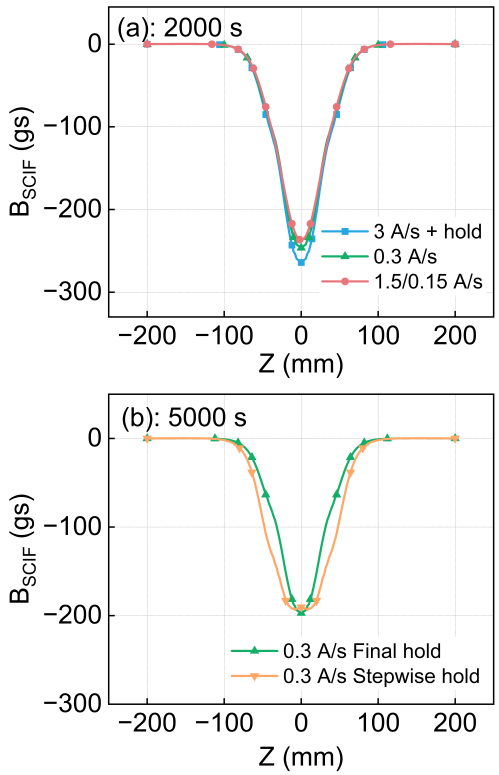

Figure 4: Spatial distribution of B_{SCIF} along the longitudinal direction. (a) Three 960 s excitation profiles at t = 2000 s. (b) Final holding and stepwise intermediate holding at t = 5000 s.

Figure 4 shows the corresponding spatial distributions of B_{SCIF}. The three profiles in Fig. 4(a) produce similar distributions, with differences mainly near the field center. Figure 4(b) shows that stepwise holding gives a broader negative SCIF region than final holding, although the central field deviations are comparable. This indicates that the charging history also affects the spatial distribution of the induced field.

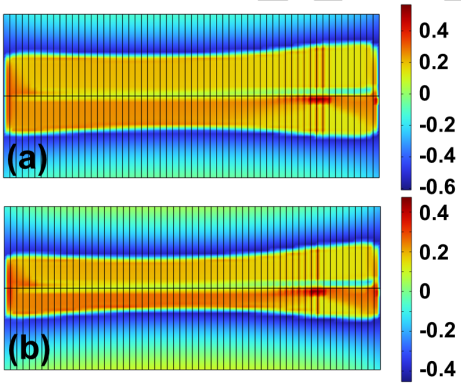

Figure 5: Evolution of the normalized screening-current density distribution $J_{\mathrm{sc}}/J_{\mathrm{cB}}$ in the HTS region for the 0.3 A/s excitation profile. (a) t = 960 s. (b) t = 5000 s.

Figure 5 shows the normalized screening-current density distribution for the 0.3 A/s excitation profile. From t = 960 s to t = 5000 s, the screening current decreases but remains non-uniform, illustrating its gradual relaxation in the ReBCO conductor.

Overall, the results show that the screening-current behavior depends strongly on the charging history. Under the present conditions, final holding at the operating current is more effective in reducing the residual screening current than a slow final ramp or distributed intermediate holding.

CONCLUSION

Screening-current effects in a ReBCO HTS bending magnet for the Hefei Advanced Light Facility were investigated using the H-formulation. Several current excitation profiles were compared to clarify the influence of charging history on screening-current relaxation and the resulting induced-field distribution. The results show that the residual screening current depends strongly on the excitation profile. A holding stage at the operating current promotes screening-current relaxation, whereas a slow final ramp or distributed intermediate holding stages do not show a clear advantage under the present conditions. These findings provide guidance for optimizing charging schemes for future ReBCO HTS bending magnets in storage-ring light sources.

ACKNOWLEDGEMENTS

This work was supported by the Research Start-up Fund for Introduced Talents of the University of Science and Technology of China (No. KY2310000052) and the USTC Bihe Youth Program for Interdisciplinary Innovation (BH-202510).

REFERENCES

[1] J. Xia *et al.*, "Design of superconducting bending magnets and an integral compensation method for the hefei advanced light facility", *Nucl. Instrum. Methods Phys. Res. A*, vol. 1082, p. 171044, 2026. doi:10.1016/j.nima.2025.171044

[2] K. L. Kim *et al.*, "Study on elimination of screening-current-induced field in pancake-type non-insulated hts coil", *Supercond. Sci. Technol.*, vol. 29, no. 3, p. 035009, Feb. 2016. doi:10.1088/0953-2048/29/3/035009

[3] Y. Yan, Y. Li, and T. Qu, "Screening current induced magnetic field and stress in ultra-high-field magnets using rebco coated conductors", *Supercond. Sci. Technol.*, vol. 35, no. 1, p. 014003, Dec. 2021. doi:10.1088/1361-6668/ac392b

[4] V. M. R. Zermeño and F. Grilli, "3d modeling and simulation of 2g hts stacks and coils", *Supercond. Sci. Technol.*, vol. 27, no. 4, p. 044025, Mar. 2014. doi:10.1088/0953-2048/27/4/044025

[5] J. Park *et al.*, "Estimation of screening current induced field on short period planar hts undulator", *IEEE Trans. Appl. Supercond.*, 2023. doi:10.1109/tasc.2023.3262616